JOURNAL OF Materials CHEMISTRY

Molecular rectification with M|(D–σ–A LB film)|M junctions

Alan C. Brady,[a] Benjamin Hodder,[a] A. Scott Martin,[b] J. Roy Sambles,[a] Christopher P. Ewels,[c] Robert Jones,[a] Patrick R. Briddon,[d] Abdalla M. Musa,[e] Charles A. Panetta[f] and Daniell L. Mattern[f]

[a]*School of Physics, University of Exeter, Exeter, UK EX4 4QL*
[b]*Current address : CSIRO Division of Telecommunication and Industrial Physics, Bradfield Road, West Lindfield, NSW 2070, Australia*
[c]*CPES, Sussex University, Brighton, UK BN1 9QJ*
[d]*Department of Physics, University of Newcastle, Newcastle, UK NE1 7RU*
[e]*Current address : Department of Chemistry and Physics, Southeastern Louisiana University, Hammond, Louisiana 70402 USA*
[f]*Department of Chemistry, University of Mississippi, University, MS 38677 USA*

Received 17th March 1999, Accepted 20th May 1999

Molecular materials of the form electron donor–sigma-bridge–electron acceptor (D–σ–A) have been synthesized and incorporated into non-centrosymmetric Langmuir–Blodgett (LB) multilayer structures. Electrical characterization has been performed using a metal|(Z-type LB film)|metal (M|LB|M) junction construction. Current density–voltage data demonstrate striking rectification behaviour. Computational modelling of the electronic structure of the material has been carried out using a first principles, density functional approach. Possible conduction mechanisms are discussed with reference to the results of this modelling.

Introduction

The inspiration for the present study is the well known paper by Aviram and Ratner,[1] in which it is proposed that a suitably engineered molecule which has a good electron donor D and a good electron acceptor A separated by a σ-bonded bridge could act as a molecular rectifier.

Previously we have presented data demonstrating molecularly controlled electrical rectification using the zwitterionic material $C_{16}H_{33}$γQ3CNQ[2] (**1** in Fig. 1). In this study, we have moved a step closer to the original Aviram and Ratner system by measuring the electrical response of a D–σ–A material, OHAPy-C-DNB (**2**). In addition we go on to theoretically model the system. Previous attempts to model σ-bridged donor–acceptor molecules[3] were based on semi-empirical techniques. In this work we model the D–σ–A molecule using a first principles density functional code, AIMPRO.[4] This includes a full structural relaxation of the 67 atom molecule, both in isolation, and in the presence of an applied field. We examine the effect of sweeping this field on the structural and electronic properties of the molecule.

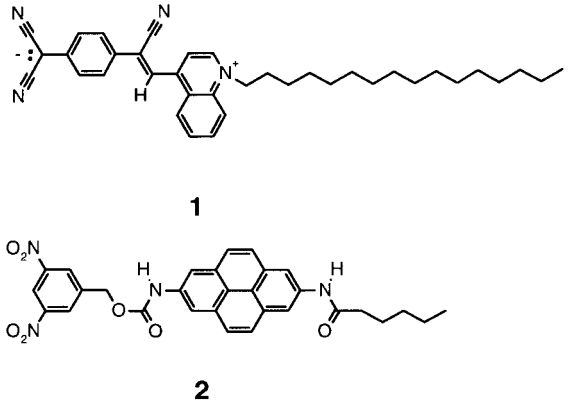

1

2

Fig. 1 Molecular structure of $C_{16}H_{33}$-γQ3CNQ (**1**) and OHAPy-C-DNB (**2**).

It is reasonable to suppose that the construction of a molecular diode would be a definitive achievement in Molecular Electronics,[5] inasmuch that conventional device behaviour would be emulated by designing the intrinsic properties of a single molecule. In view of the fact that the results presented here are for a σ-bridged moiety, that no hysteresis is recorded, and that molecular modelling is able to explain the behaviour, this work is a major step towards establishing the foundations of molecular rectification.

Experimental

Molecular synthesis

The D–σ–A molecule 3,5-dinitrobenzyl 7-(1-oxohexylamino)-pyren-2-ylcarbamate (OHAPy-C-DNB) (**2**) was prepared using the synthesis outlined in Fig. 2. The donor group, ethyl 2-aminopyrene-7-carboxylate (**3**),[6] was acylated with hexanoyl chloride to provide amide **4**. The C_6 amide tail was included to facilitate LB film formation. After hydrolysis, a Curtius rearrangement procedure[7] was used to convert the carboxylic acid **5** to the isocyanate **6**. Addition of the acceptor dinitrobenzyl alcohol converted **6** to the σ-bridged carbamate **2**.

Ethyl 7-(1-oxohexylamino)pyrene-2-carboxylate (4). To a solution of the hydrochloride salt of **3** (0.500 g, 1.54 mmol) and triethylamine (0.363g, 3.59 mmol) in 50 ml of CH_2Cl_2 was added dropwise at 0 °C a solution of hexanoyl chloride (0.207 g, 1.54 mmol) in CH_2Cl_2. After three hours, the mixture was treated with 5% HCl and extracted with CH_2Cl_2. Drying over $MgSO_4$ and evaporation of the solvent, followed by recrystallization from EtOH, afforded off-white crystals in 85% yield, mp 229–231 °C; IR (KBr) 3285, 3050, 2932, 2871, 1715, 1654, 1540, 1388 cm^{-1}; ^{1}H-NMR ($CDCl_3$) δ 8.85 (2H, s), 8.40 (2H, s), 8.15 (2H, d), 8.05 (2H, d), 7.75 (1H, s), 4.05 (2H, t), 2.50 (2H, t), 1.85 (2H, m), 1.50 (3H, t), 1.45 (4H, m), 0.95 (3H, t). Anal. Calcd for $C_{25}H_{25}NO_3$: C, 77.50; H, 6.50; N, 3.62. Found: C, 77.46; H,6.38; N, 3.55%.

7-(1-Oxohexylamino)pyrene-2-carboxylic acid (5). A solution of **4** (0.300 g, 0.774 mmol) in 100 ml of EtOH was added

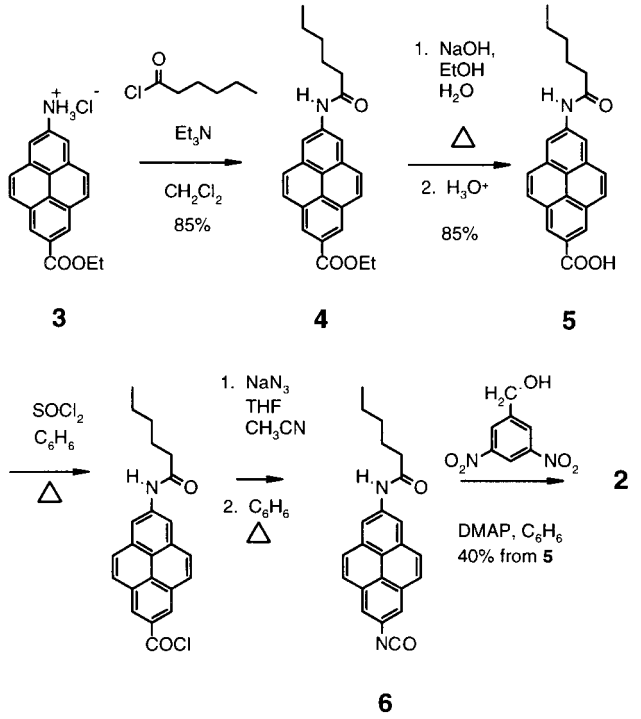

Fig. 2 Synthesis of **2**.

to NaOH (3.00 g, 75.0 mmol) in 50 ml of water. The mixture was heated on steam until all of the starting compound dissolved. Acidification of the hot solution gave, after cooling, an 85% yield of **5**: mp 340 °C (decomp.); IR (KBr) 3304, 3050, 2951, 2881, 1685, 1676, 1648, 1540, 1388 cm^{-1}; ^{1}H-NMR (DMSO-d_6) δ 10.5 (1H, s), 8.85 (2H, s), 8.60 (2H, s), 8.30 (2H, d), 8.15 (2H, d), 2.45 (2H, t), 1.70 (2H, m), 1.40 (4H, m), 0.90 (3H, t). Anal. Calcd for $C_{23}H_{21}NO_3$: C, 76.86; H, 5.89; N, 3.90. Found: C, 76.84; H, 5.83; N, 3.90%.

3,5-Dinitrobenzyl 7-(1-oxohexylamino)pyren-2-ylcarbamate (2). Into a flask equipped with a reflux condenser and a $CaSO_4$ drying tube were placed 0.27 g (0.76 mmol) of **5** in 20 ml of dry benzene and 1 ml of $SOCl_2$. After 8 h of heating at reflux, IR showed complete conversion to the acid chloride (1752 cm^{-1}). Rotary evaporation gave an oil which was treated with sodium azide (0.230 g, 3.57 mmol) and 1:1 CH_3CN–THF. After stirring overnight, IR showed complete conversion to the acyl azide (2142 and 1684 cm^{-1}). The mixture was filtered and the solvent was removed by rotary evaporation to give 0.25 g (0.65 mmol) of solid acyl azide, which was heated at reflux in 25 ml of dry benzene for 24 hours to complete the Curtius rearrangement to **6**. IR showed complete conversion to isocyanate (2259 cm^{-1}). 3,5-Dinitrobenzyl alcohol (0.13 g, 0.65 mmol) and dimethylaminopyridine (DMAP) (40 mg, 0.33 mmol) were added. After 2 hours at room temperature, IR showed complete conversion to carbamate (1740 and 1604 cm^{-1}). The solvent was removed by rotary evaporation and the residue was crystallized from toluene to give a 40% yield of **2**: mp 240 °C (decomp.); IR (KBr) 3378, 3112, 2954, 2929, 2869, 1740, 1647, 1604, 1540, 1384 cm^{-1}; ^{1}H-NMR (DMSO-d_6) δ 10.55 (1H, s), 10.40 (1H, s), 8.80 (3H), 8.50 (2H, s), 8.35 (2H, s), 8.10 (4H, s), 5.50 (2H, s), 2.45 (2H, t), 1.70 (2H, m), 1.40 (4H, m), 0.90 (3H, t). Anal. Calcd for $C_{30}H_{26}N_4O_7$: C, 64.97; H, 4.73; N, 10.10. Found: C, 64.34; H, 4.41; N, 9.86%.

Junction fabrication

Fig. 3 shows a surface-pressure–area isotherm of **2** recorded on a standard rectangular PTFE trough with the moving barrier compressing the film at 0.5 cm^2 s^{-1}. The measured

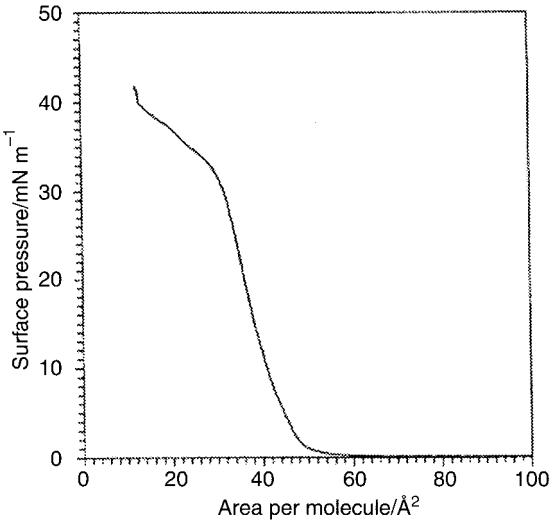

Fig. 3 Surface-pressure *vs.* area isotherm of **2**.

take-off and collapse areas are in agreement with the calculated cross-sectional areas of the molecule lying flat and standing upright respectively.

Junction fabrication remains essentially the same as Geddes *et al.*[8] Silicon (110) wafers, were cut into ~20 mm × 20 mm squares, and rendered hydrophobic in a solution of 2% dimethyldichlorosilizane in 1,1,1-trichloroethane. A planar base electrode consisting of 100 nm thick 99.99% pure silver was then thermally evaporated onto the silicon. Langmuir–Blodgett (LB) deposition onto the substrates was performed within one hour of removal from vacuum in order to minimize the sulfidization of the silver.

The Langmuir monolayer was spread from a solution of ~1 mg solute in 100 ml ARISTAR (Merck) grade chloroform, and was observed to be colourless and stable over many hours. LB transfer was conducted at a surface pressure of 25 mN m^{-1}, using a dipping speed of 0.1 mm s^{-1}, and with a 20 second delay incorporated into the dipping routine between each stroke to allow for monolayer relaxation. Under these conditions, the LB transfer occurred on the up-stroke only, *i.e.* Z-type deposition. The resultant transferred monolayer therefore has the molecules oriented with the pyrene backbone upright, with the hydrophilic dinitrophenyl acceptor groups closest to the silver base electrode. The short aliphatic tail on this molecule means that it has only weak amphiphilic nature; consequently there is unlikely to be a strong overturning force acting on subsequent (alternate) layers.

The samples were then desiccated at atmospheric pressure for at least two weeks to remove trapped water and to allow some annealing of the LB film.

Electrical characterisation

Filled figure-8 shaped magnesium pads (area 0.8 mm^2) of apparent thickness 200 nm were deposited onto the film at an apparent rate of ~0.5 nm s^{-1} (these values are uncertain due to the unpredictable nature of magnesium deposition[9]). The use of a reactive metal for the top electrode has been questioned, but it has been unequivocally demonstrated that this does not influence the electrical measurements.[10]

Without breaking the vacuum, 6 nm thick silver circles were deposited onto the centre of both annular limbs of each magnesium pad. Contact to the base electrode was made with silver paste, whilst connection to top electrodes was made with thin gold wires which were positioned above the silver pads, the gap being bridged using droplets of gallium–indium eutectic.

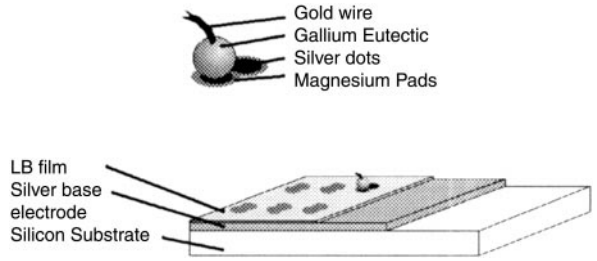

Fig. 4 Schematic of junction construction.

This geometry is depicted in Fig. 4. Electrical measurements were recorded by applying a voltage with a triangular waveform between the base electrode and top electrode (which is regarded as zero potential).The current passed by the junction was measured using an electrometer.

Ab initio molecular modelling

These model calculations were performed using the serial version of AIMPRO, a local density functional code. In this code, the electronic wave-functions are expanded in real-space using s- and p-Gaussian orbitals centered at atomic nuclei. Norm-conserving pseudo-potentials[11] are used in order to exclude core electrons. The self-consistent energy E and the force on each atom are calculated, and the atoms moved by a conjugate gradient algorithm to equilibrium.

At this point electric field gradients can be incorporated into the calculation. An 'initial guess' structure was constructed using the 'Builder' module of the 'Insight II' code from MSI.[12] This structure was then fully relaxed using AIMPRO. As the electric field was varied, the structure was again allowed to fully relax at each field point. The Kohn–Sham (K–S) levels give only a semi-quantitative description of donor and acceptor levels—for this reason, examination of the K–S eigenvalues should only be used for qualitative analysis of the system, and not for direct comparison with experiment. The self consistent energy E and force on an atom were evaluated while a constant electrical field, defined such that a positive field was one that ran from the acceptor group towards the donor group, acted on the molecule; the molecule was then relaxed using these forces. The externally applied experimental fields may not exactly match those felt by individual molecules for a number of reasons, due to for example, screening effects. In addition, variations in the surface roughness of the metal films can lead to locally increased fields.

These calculations were initially performed with spin averaged wavefunctions, and then repeated using spin polarisation with little overall effect. We fully relaxed the structure in the zero field constraint, and then varied the applied field with no relaxation. We then repeated the procedure but allowed the molecule to fully relax in the presence of the field at each point.

Results and analysis

UV–visible spectra measured for LB films deposited on silica were qualitatively identical to those measured in solution. There are no peaks in the spectra corresponding to intramolecular charge transfer. Furthermore the peak absorbances from the solid samples scale linearly with number of LB layers. This suggests that there is little or no inter-layer interaction, and that LB deposition is uniform from layer to layer.

At low applied biases junctions do not exhibit noticeable non-linear behaviour and the J–V trace is a parallelogram which is used to calculate the junction capacitance and conductance. The applied bias was gradually increased, and a non-linear, asymmetric response in current flow was observed, with no hysteresis.

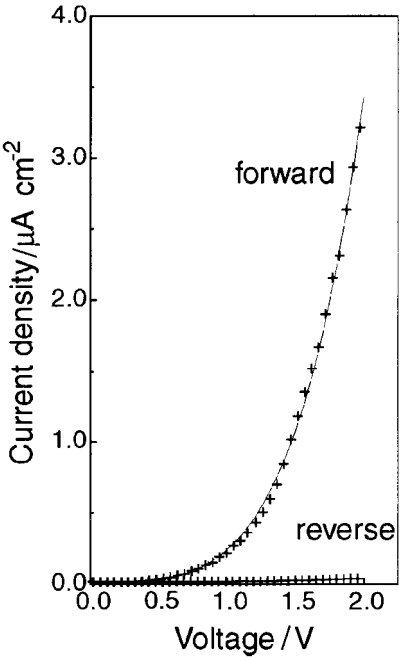

Fig. 5 Current density–voltage characteristic for a 5 layer film of OHAPy-C-DNB showing greatly enhanced forward current passage.

A current density–voltage plot for a 5 layer film is shown in Fig. 5. The forward-bias current flow corresponds to electron transfer in the direction corresponding to magnesium to pyrene (donor) and dinitrophenyl (acceptor) to silver. Fig. 6 shows data from the same junction in which the maximum negative voltage has been increased to allow analysis of the reverse bias current. It can clearly be seen that the asymmetric response is not simply an artifact of a voltage offset induced by the difference between the work-functions of the electrodes.

A measure of the J–V trace asymmetry is the 'rectification ratio' defined as in eqn. (1).

$$\text{Rectification ratio} = \frac{I_{\text{forward}}}{I_{\text{reverse}}} \quad (1)$$

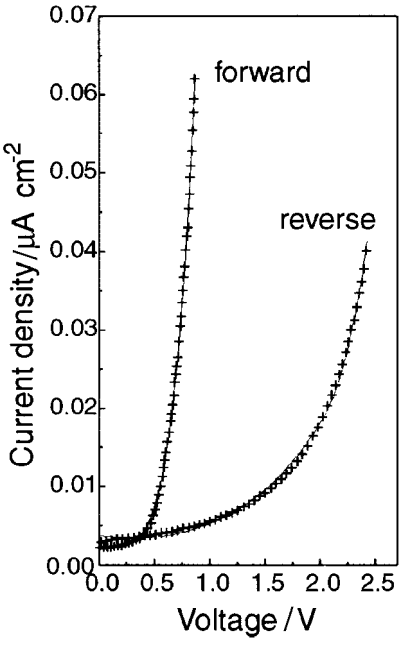

Fig. 6 Current density–voltage curve in which the applied voltage signal has been offset by −0.78 V so that the forward and reverse currents were of comparable magnitude.

for a given magnitude of voltage. This value increases with applied bias amplitude, and reaches 130 just before junction breakdown at a bias of $\sim$2.5 V. However, *the high current flow is in the opposite direction* to the Aviram and Ratner model.

There exist numerous models for conduction mechanisms through thin insulating films. These are generally characterised by simple mathematical functions, which can be used as an indication of the dominant process occurring in a junction.

Reverse bias data fits well a combination of an ohmic (linear) term (calculated from low bias data) and an exponential term [eqn. (2)]:

$$J = a_0 + a_1 V + a_2 e^{(a_3 V)} \quad (2)$$

The exponential component in eqn. (2) is attributed to Poole-type conduction,[13] which has been observed under reverse bias for several systems, including both zwitterionic and 'bleached' forms of **1**, and more recently in non-centrosymmetric LB film of ω-tricosenoic acid.[14] In all cases we associate the reverse bias behaviour with the structural asymmetry of the LB film. This is clearly demonstrated with the insulating material, ω-tricosenoic acid. As a symmetric (Y-type) LB film this produces symmetric J–V data, but when deposited as a Z-type film, the J–V trace becomes asymmetric. It is conjectured that such a response is due to electron conduction involving asymmetric Poole centres (*i.e.* an asymmetric distribution of electronic trap sites), which would be plausible if the Poole centres reside at fixed sites on the molecules. This is consistent with the results presented here; fitting the new data to eqn. (2) gives a Poole centre separation which is comparable to a single molecular length.

Forward bias behaviour could not be explained using an exponential, but instead was found to follow a dependence of the form shown in eqn. (3).

$$J = b_0 + b_1 V + b_3 V^3 + b_5 V^5 \quad (3)$$

The V^5 component, although dominant, was insufficient on its own—the lower odd terms needed to be included to fully fit the data.

It is interesting to compare the V^5 response with the V^3 response that was previously

$$J = c_0 + c_1 V + c_3 V^3 \quad (4)$$

measured in M|DπA zwitterion (**2**)|M junctions [eqn. (4)] using an identical experimental geometry.

It is tempting to suggest that assisted tunnelling through molecular orbitals can be characterised by a non-linear expansion of the form given in eqn. (5)

$$J = J_0 + \sum_{i=1}^{\infty} n_{2i-1} V^{2i-1} \quad (5)$$

where the coefficients n_{2i-1} will depend on aspects of the molecular orbital structure.

Whilst the measured response will be a convolution of the molecular behaviour and the coupling between the molecular orbitals adjacent to the interface and the surface states of the electrodes, the non-exponential behaviour suggests that there is a field dependent assisted tunnelling mechanism which is molecular in origin. In order to understand the present result, we turn to molecular modelling.

It would be very useful to be able to accurately model the whole system, taking into account the interactions between the molecule and the electrode, and between neighboring molecules in the LB film. The important first step is to understand the electronic structure of the molecule, and how this interacts with large external electric fields.

The Kohn–Sham (K–S) eigenvalues obtained from AIMPRO are shown in Fig. 7. The localisation of these is shown on the plot; levels localised primarily on the dinitrobenzyl acceptor group are shown as solid, and those on the pyrene donor group as dashed lines. Unpopulated levels are shown using shorter lines than populated levels. The donor–acceptor structure of the molecule is clearly apparent; the K–S level corresponding to the highest occupied molecular orbital (HOMO) is localised on the pyrenylcarbamate, and the K–S level corresponding to the lowest unoccupied molecular orbital (LUMO) on the dinitrobenzene. This calculation shows that the material behaves like a semiconductor in which the band gap of 0.8 eV varies as an electric field is applied.

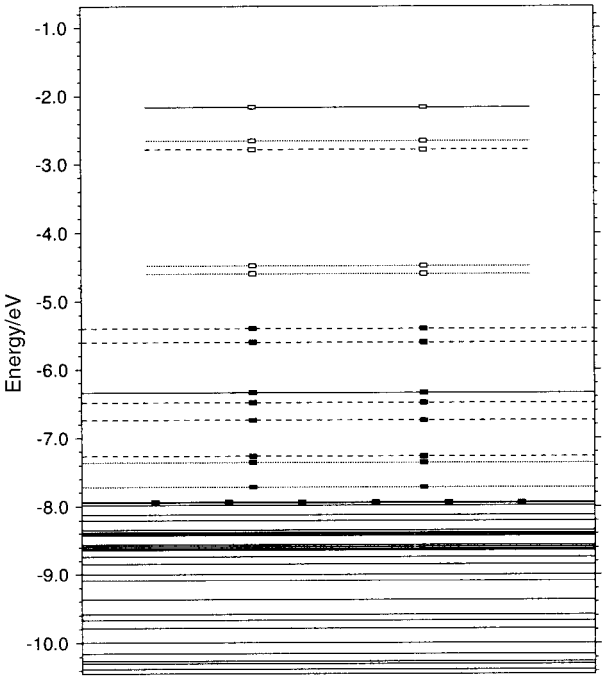

Fig. 7 Kohn–Sham eigenvalues for the relaxed DσA, with no applied field. Shorter lines/empty boxes show unoccupied levels. For levels near to the 'molecular band-gap', solid lines indicate the level is localised on the dinitrobenzyl acceptor group, dashed lines indicate localisation on the pyrene donor group.

In Fig. 8 the variations of the K–S HOMO and K–S LUMO levels with field are plotted; the K–S LUMO varies greatly with field whereas the K–S HOMO shows much less variation.

The variation with field of the K–S HOMO–LUMO gap is shown in Fig. 9. There is a pronounced curvature at high positive fields due to the anti-crossing effect as the two levels approach one another.

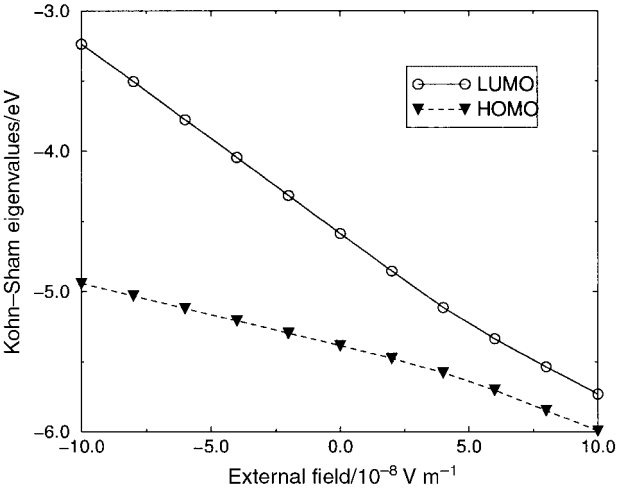

Fig. 8 Variation in the Kohn–Sham eigenvalue for the HOMO and LUMO of the relaxed DσA molecule with applied field.

Discussion

The structure rectifies, and does so in a manner counter to that predicted by a simple Aviram and Ratner type energy level model. The mismatch of the electrode work functions cannot be responsible as previous studies have shown that 'inactive' molecules in this type of configuration do not rectify. Furthermore, the functional forms of the forward and reverse bias data are quite distinctly different, indicating that the response is not just symmetric about some offset voltage.

Instead we need to find a molecular process which could account for the rectifying behaviour.

Molecular conduction involves both intermolecular and intramolecular charge transfer. Electron transfer to and from the electrodes occurs *via* resonant tunnelling due to the overlap of the surface states of the electrode and the tail of molecular states with energy close to Fermi edge of the metal.

We infer from the molecular modelling that the HOMO–LUMO gap varies as the very high electric fields distort the molecular wavefunctions. As the HOMO–LUMO gap closes, the excited state becomes more accessible. The charge distribution of the resulting intermediate, $M(-)|\cdots D^+\sigma A^-\cdots|M(+)$, is stabilized, whereas this state would be destabilized under reverse bias $M(+)|\cdots D^+\sigma A^-\cdots|M(-)$. Due to the increased HOMO–LUMO energy gap under reverse bias (Fig. 9), the alternative excited state $M(+)|\cdots D^-\sigma A^+\cdots|M(-)$ is also inaccessible.

The narrowing of the HOMO–LUMO gap in the electric field gradient has the effect of increasing the probability of intermolecular charge transfer by lowering the effective energy of the next molecule in the chain with respect to an occupied state of a donor molecule. Furthermore, the lowering in energy of unoccupied states under forward bias increases the overlap of the silver Fermi edge with the LUMO of the neighbouring molecules, and hence increases the resonant tunnelling probability from A^- to silver.

In summary, the convergence of the HOMO and LUMO energy levels under forward bias provides a conduction pathway through the multilayer which is not available in the Aviram and Ratner formulation. The contrasting increase in the HOMO–LUMO gap under reverse bias leads to an asymmetry in electron transfer and resonant tunnelling processes. This asymmetry is purely due to the architecture of a single molecule, and can hence be justifiably described as molecular rectification.

Conclusion

A molecular donor–σ-bridge–acceptor compound, similar to that described in Aviram and Ratner's seminal molecular rectifier proposal, has been synthesized and incorporated into a junction. Measured *J–V* curves have exhibited high rectification ratios in excess of 100 before breakdown and display no hysteresis. However, the direction of high current flow is in the opposite sense to that suggested by Aviram and Ratner's model.

The electrical behaviour under both bias senses has been compared closely with simple functional dependences. Reverse bias is characterised by a dominant exponential that has been interpreted as Poole conduction, with the characteristic Poole centre separation calculated to correspond to molecular dimensions. Under forward bias the *J–V* response does not conform to conventional hopping models, but follows a non-linear expansion which is believed to be characteristic of conduction through molecular orbitals.

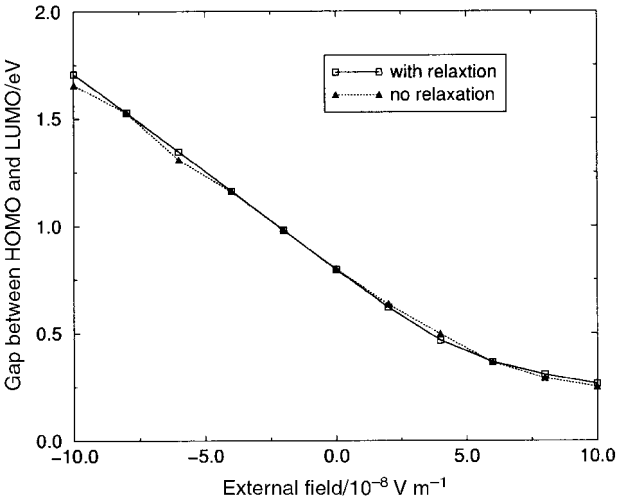

Fig. 9 Gap between the donor HOMO and acceptor LUMO levels for DσA under applied field. It can be seen that allowing full structural relaxation does not appreciably alter the gap.

Ab initio modelling of the material has provided an electronic structure and shown an electric-field dependent variation of the HOMO–LUMO gap which we propose leads to the molecular rectification effect.

Acknowledgements

The authors gratefully acknowledge the support of the EPSRC (UK), and NSF-EPSCoR and the State of Mississippi (USA).

References

1 A. Aviram and M. Ratner, *Chem. Phys. Lett.*, 1974, **29**, 277.
2 G. J. Ashwell, J. R. Sambles, A. S. Martin, W. G. Parker, M. Szablewski, *J. Chem. Soc., Chem. Commun.*, 1990, **19**, 1374.
3 A. Broo and M. C. Zerner, *Chem. Phys.*, 1995, **3**, 407; A. Broo and M. C. Zerner, *Chem. Phys.*, 1995, **3**, 423.
4 R. Jones, and P. R. Briddon, in *Identification of Defects in Semiconductors*, ed. M. Stavola, Academic Press, New York, 1998, ch. 6.
5 D. H. Waldeck and D. N. Beratan, *Science*, 1993, **261**, 576; R. M. Metzger and C. A. Panetta, *New J. Chem.*, 1991, **15**, 209; D. Bloor, *Phys. Scr.*, 1991, **T39**, 380; C. A. Mirkin and M. A. Ratner, *Annu. Rev. Phys. Chem.*, 1992, **43**, 719.
6 A. Musa, B. Sridharam and D. L. Mattern, *J. Org. Chem.*, 1996, **61**, 5481.
7 R. M. Metzger, *Langmuir*, 1990, **6**, 350. R. M. Metzger, D. C. Wiser, R. K. Laidlaw, M. A. Takassi, D. L. Mattern and C. A. Panetta, *Langmuir*, 1990, **6**, 350.
8 N. J. Geddes, J. R. Sambles, D. J. Jarvis and W. G. Parker, *Appl. Phys. Lett.*, 1990, **56**, 1916.
9 N. J. Geddes, J. R. Sambles and D. J. Jarvis, *Thin Solid Films*, 1988, **167**, 261.
10 A. S. Martin, J. R. Sambles and G. J. Ashwell, *Phys. Rev. Lett.*, 1993, **79**, 218.
11 G. B. Bachelet, D. R. Hamann and M. Schlüter, *Phys. Rev. B*, 1982, **26**, 4199.
12 Insight II version 95.0 Molecular Modelling System, Copyright © 1995 BIOSYM/MSI, BioSym Technologies.
13 R. M. Hill, *Philos. Mag.*, 1971, **23**, 59.
14 A. S. Martin and J. R. Sambles, *Nanotechnology*, 1996, **7**, 401.

Paper 9/02107H